USE OF EBSD TO STUDY HYDROGEN INDUCED CRACKING IN PIPELINE STEEL

V. Venegas[a], F. Caleyo[a]; J. L. González[a], T. Baudin[b], J. M. Hallen[a] & R. Penelle[b]
[a] Departamento de Ingeniería Metalúrgica, Instituto Politécnico Nacional, México D.F. 07738, México.
[b] Laboratoire de Physico-Chimie de l'Etat Solide, Université de Paris Sud, Orsay 91405, France.

ABSTRACT

The spatial distribution of plastic deformation and grain orientation surrounding hydrogen induced cracks is investigated in samples of API-5L-X46 pipeline steel using scanning electron microscopy and electron backscattering diffraction (EBSD). This work shows direct experimental evidence of the influence of microstructure, microtexture and mesotexture on HIC crack path.

1 INTRODUCTION

Hydrogen induced cracking (HIC) is a major problem in low strength carbon steels with ferrite and pearlite microstructure such as API 5L pipeline steels. Although it is well established that nonmetallic inclusions are favorable sites for HIC, divergent theories have been put forward to explain the microscopic behavior of this phenomenon. In this sense, the most common theories are those of decohesion, hydride formation, enhanced plastic flow and transport models (Birnbaum [1]). All these mechanisms are based on the fact that hydrogen damage in metals is greatly influenced by the presence of defects which act as hydrogen trapping sites such as grain boundaries, dislocations and inclusions. However, the influence of microstructure on the propagation path of the HIC cracks is still on debate; especially on the identification of the mechanisms responsible for the low resistance paths to crack propagation and interconnection.

The electron backscattering diffraction (EBSD) technique makes possible to relate the spatial distribution of plastic deformation to microstructural features in a wide variety of materials (Schwartz *et al.* [2]). The use of this technique allows to achieve a better understanding of the mechanisms responsible for the fracture of materials and therefore to improve the methods for the identification of in-service materials at high risk of failure. Nevertheless, an extended application of the EBSD in engineering fracture mechanics is still missing. In the case of HIC, this technique seems particularly useful to investigate: (i) the strain fields surrounding hydrogen induced cracks, (ii) the influence of plastic deformation and shear stress distribution on the crack propagation path and (iii) the influence of microstructure and local texture on the crack propagation path. It is important to underline that no other technique is currently available for mapping strain fields with the combined high resolution and dynamic range in size of the imaging area offered by EBSD.
This paper describes a study on the influence of microstructure, local texture and grain boundary distribution on HIC in samples of API-5L-X46 pipeline steel using EBSD. Experimental evidence of the influence of microtexture and grain boundary distribution (mesotexture) on HIC propagation path is presented and from that, the characteristics of the HIC mechanism are discussed.

2 EXPERIMENTAL

Plates taken from an in-service sour gas API-5L-X46 pipeline that experienced HIC were cut as shown in Fig. 1a. In this figure, AD, RD and CD represent the axial, radial and circumferential directions of the pipe, respectively. The samples were first polished to a 0.05 μm finish and then

electropolished for two minutes in a 90% ethanol - 10% perchloric acid mixture at -70°C and 30V. Orientation imaging microscopy (OIM^{TM}) (Schwartz *et al.* [2]) was used to produce orientation and strain maps over an area of 450 μm (CD) × 430 μm (RD) in a sample showing HIC. Individual orientations were automatically measured using EBSD on a hexagonal grid with a 2 μm step size in a Karl-Zeiss DSM 940 SEM. The amount of deformation associated with each point in the OIM microstructure was approximated from the quality parameter IQ of the corresponding EBSD patterns. The IQ values were scaled using the minimum and maximum IQ observed and used as a relative measure of the local strain. Grain boundaries were defined by the presence in the orientation maps of point-to-point disorientations greater than 2°. They were classified into: (i) coincidence site lattice boundaries (CSL Σ) with a maximum permissible deviation of $15°/\Sigma^{1/2}$, (ii) low-angle boundaries (LABs or Σ1) and (iii) high-angle disordered boundaries (HABs or Σ>33). The crystallographic features of the crack propagation paths were investigated based on the orientation relationship between the shear/cleavage surfaces of the cracks and the crystallographic planes of the surrounding grains.

3 RESULTS AND DISCUSSION

Figure 1b shows a SEM micrograph of the studied sample after etching with Nital. The sample shows the pearlite/ferrite microstructure typical of low strength carbon steels. Using the linear intercept method, the average grain size was estimated to be 20 μm. HIC appears in the form of stepwise cracks parallel to the pipe wall. The HIC cracks grow both intergranular and transgranular. In this specimen, ferrite/pearlite and inclusion/matrix interfaces provide crack propagation paths only in a few cases. Another feature to emphasize is that all the crack ends deflect toward the radial direction which shows the high degree of interaction between these cracks.

Although a quantitative analysis of the local crystallographic texture is not relevant for this study, the analysis of the OIM orientation maps of the investigated sample evidenced two important facts: (i) the sample has a non-preferential local texture with components of moderate-

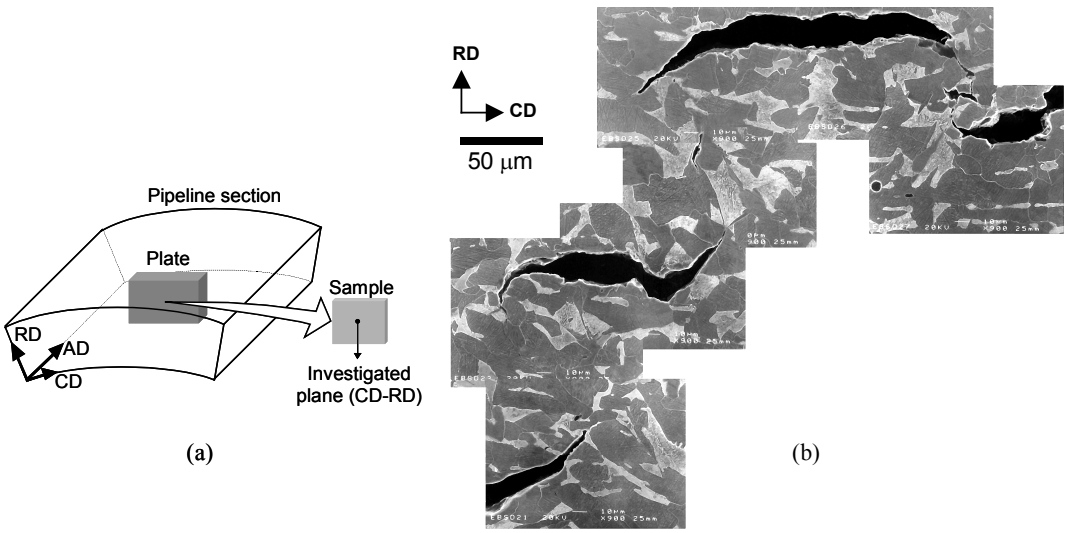

Figure 1. (a) Sample selection process. (b) SEM micrograph of the sample containing HIC cracks.

to-low strength and (ii) orientations do not cluster so that there is not a dominance of crystallographic-induced paths for crack growth or arrest.

The strain diminishes the quality of the EBSD patterns because of the lattice bending and the corresponding spread in the Bragg scattering angle in the diffracting volume. In the OIM data, this is reflected in the quality parameter IQ related to the site where the EBSD patterns are produced. Therefore, the EBSD image quality map, or simply IQ map, can be interpreted as an indirect measure of the spatial distribution of strain fields in the material (Schwartz *et al.* [2]). The IQ map of the studied sample is shown in Fig. 2a in which the darkness increases with the decrement of the IQ value. This figure shows that strain fields surround the cracks and connect them in a stepwise manner. This is a direct experimental evidence of the presence of the shear stress fields that connect the HIC crack tips. It is important to emphasize that the regions with low quality EBSD patterns in Fig. 2a are not related to specific grain orientations but only to the strain fields that surround and connect the cracks. Therefore, the dependence of IQ on orientation was not taken into account here.

Figure 2a clearly shows that the most intense plastic zones are located between the approaching cracks and near to crack edges and tips. Quantitatively, this is confirmed by the high values of the strain intensity factor, expressed as 1-IQ, found at these regions. Figs. 2b-2e show the variation of the strain intensity along the radial directions R1, R2 and R3 (indicated in Fig. 2b). The 1-IQ values decrease more than 70% for an average distance of 7μm from crack edges. This distance is assumed to be the average extension of the strain field in the pipe's RD. In the case of direction

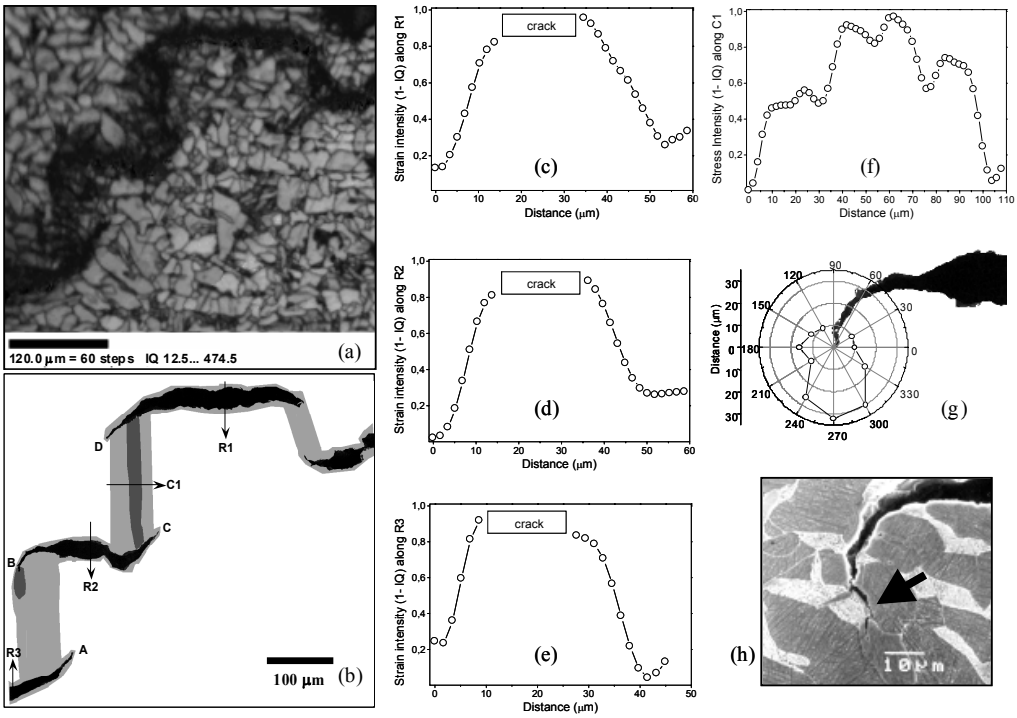

Figure 2. (a) EBSD image quality map (IQ map) of the studied sample. (b) Schematic illustration of the strain fields surrounding the cracks. (c-f) Strain intensity measured as 1-IQ along the directions indicated in (b). (g) Extension of the strain field surrounding crack tip B. (h) Detail of crack tip B.

C1, which is parallel to the pipe's AD, the variation in strain intensity shows that the deformation zone along this direction is about 90 μm wide. This zone, and that between crack tips A and B, are affected by the shear stress resulting from the interaction between the approaching cracks.

On the other hand, the strained zones at crack tips A, C and D in Fig. 2a do not show a significant increase in their extension with respect to the extension of the strained zone at crack edges. This can be attributed to the presence of suitable oriented slip planes in the crack path that favor the relaxation of the shear stress at these tips by plastic deformation. In contrast, the polar diagram in Fig. 2g shows that the strained zone around tip B extends up to 30 μm downward in the pipe's RD. This difference can be attributed to the fact that at tip B, the material does not crack through slip planes as in tips A, C and D so that high stresses develop at this point. A detailed observation of tip B shows that this crack grows closely parallel to a ferrite/pearlite interface and then stops at a ferrite grain (Fig. 2h).

These results prove that HIC strongly depends on crystallographic aspects such as the availability of suitably oriented cleavage planes, slip systems and high angle grain boundaries that provide weak interfaces for crack propagation. The EBSD technique has been used in a previous work to study the orientation of crack trace relative to the rolling plane in duplex stainless steels (Kim [3]). In other studies (Zakaria [4]), the characteristic "S" shape of the HIC cracks has been related to the effect of hydrogen pressure inside the cracks and to the presence of incoherent particles and weak interfaces that the cracks use to propagate. In this work, the orientation of the crack traces was related to the crystallographic data determined by EBSD for the grains near to crack tips in an attempt to get a better understanding of the crystallographic features of HIC.

Figure 3 shows the orientation relationship between the crack trace and the closest bcc slip system and cleavage plane for the grains at crack tips A-D. For grains 1, 5, 8 and 9, the angle

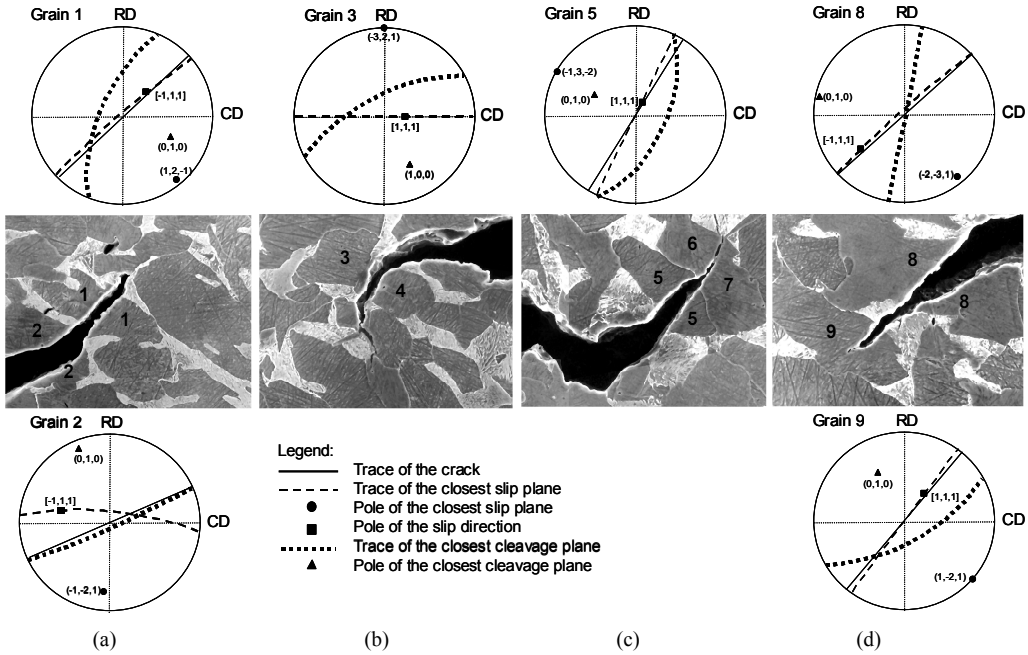

(a) (b) (c) (d)

Figure 3. Angular relationship between the trace of cracks and the slip and cleavage planes of the marked grains. (a) Crack tip A. (b) Crack tip B. (c) Crack tip C. (d) Crack tip D.

between the pipe wall and the trace of the slip plane closest to the crack plane is about 45º (42º in average; the largest deviation occurs for grain 5 for which this angle is 34º). Under this condition, it is reasonable to assume that these grains are more likely to plastically deform by shear, therefore relaxing the stresses around them and at the near crack tips. In addition, the orientation of the active slip planes in these grains determines the deviation of the planar crack paths leading to S shaped cracks (note that the presence of HABs suitably oriented such as that between grains 6 and 7 in Fig. 3c, also contributes to the propagation of the S shaped cracks). The results found for tips A, C and D agree with the decohesion mechanism found in HSLA steels with ferrite-pearlite microstructure in which decohesion along dislocation cell boundaries parallel to the activated slip planes is the main cause of hydrogen embrittlement (Naguno [5]).
However, this is not the case of tip B (Fig. 3b), for which the trace deflection that leads to the S shape occurs through a high angle boundary between grains 3 and 4. This happens because grain 3 has no cleavage planes favorably oriented for the planar propagation of this crack as occurs in grain 2 at tip A (Fig. 3a). In addition, the slip plane closest to the crack trace in this grain is oriented perpendicular to the pipe's radial direction so that slip does not activate in this case.

Figures 1 and 3 corroborate the intergranular and transgranular nature of the HIC crack propagation path in the studied material. Moreover, the results shown in Fig. 3 suggest that the distribution of grain boundaries has a noticeable influence on the way that HIC behaves. Accordingly, a total of 253 grain boundaries were investigated in the sample in order to establish the relationship between the HIC crack propagation path and the grain boundary character distribution. Fig. 4 shows the proportion of LABs, HABs and CSLs boundaries in the regions not affected by HIC (201 identifiable boundaries) and across the HIC cracks (52 identifiable boundaries). The distribution of grain boundaries in the studied sample is close to that predicted for a polycrystal with a random texture. However, the studied sample shows a higher number of LABs in both the cracked and non-cracked regions as well as a smaller number of the CSLs associated with the cracks. Not surprisingly, intergranular propagation occurs mainly through high angle boundaries while CSLs and LABs provide less than 18% of the propagation paths. This is specially true for CSLs which supply less than 5% of these paths. This agrees with the grain boundary energy classification generally accepted in which, as a rule, low energy boundaries such as low angle boundaries and low Σ CSLs are more resistant to fracture than high-energy random boundaries (Watanable [6]).

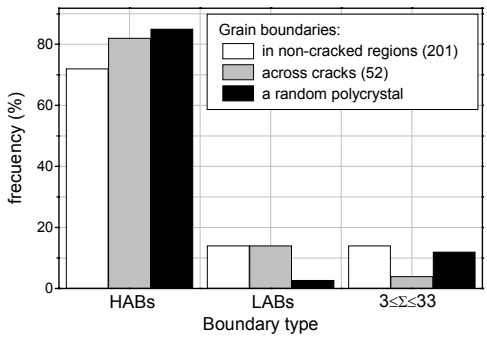

Figure 4.Grain boundary type statistic in cracked and non-cracked regions in the investigated sample. The statistic of the random oriented polycrystal is shown for the sake of comparison.

4 CONCLUSIONS

The EBSD technique have been successfully used to investigate the distribution of plastic deformation surrounding HIC cracks and the crystallographic features of HIC in a sample of API-5L-X46 steel. The following results were obtained.

The strain fields that surround and connect the HIC cracks can be evidenced experimentally by mapping the quality index of the EBSD patterns produced by the material. Intense strain regions are associated with plastic zones left in the wake of the propagation crack which extend in average 7μm from the crack edges. However, the most intense plastic zones develop between approaching cracks due to the shear stress that connect them.

The S shape of the HIC cracks can be related to the slip and cracking of grains located in the shear stressed regions between interacting cracks as well as to the crack propagation through suitably oriented high angle grain boundaries. This later mechanism activates when the crack arrests its planar propagation due to the lack of high angle boundaries or cleavage planes oriented parallel to the pipe wall while the orientation of the nearest grains in the shear stressed region does not allow crack to deflect by slip and cracking.

The paths for intergranular crack propagation in this material are mainly high angle (disordered, high-energy) grain boundaries while transgranular propagation occurs by cleavage along the {001} planes and by slip on the {112}<111> and {123}<111> systems. These results suggest the feasibility of improving the HIC resistance of pipeline steels via crystallography texture control and grain boundary engineering.

5 REFERENCES

[1] Birnbaum H.K. Environment Induced Cracking of Metals. NACE 10. pp. 21-29; 1990.

[2] Schwartz A.J., Kumar M., Adams B.L. (Eds). Electron Backscatter Diffraction in Materials Science. New York: Kluwer Academic/Plenum Publishers; 2000.

[3] Kim S. and Marrow T.J. Application of EBSD to cleavage fracture in duplex stainless steel. Scripta Mat. Vol. 40(12); pp.1395-1400; 1999.

[4] Zakaria M.Y.B. and Davies T.J. Formation and analysis of stack cracks in a pipeline steel. J Mater. Sci. Vol. 28; pp. 3322-3328; 1993.

[5] Naguno M, Miyamoto K, Kubota T. Proc. Of the 3er Int. Conf. On Effect of Hydrogen on Behavior of Materials. The Met. Soc. of ASME. pp. 331-339; 1980.

[6] Watanabe T. Grain Boundary Design for advance materials on the basis of the relationship between texture and GBCD. Texture and Microstructures. Vol. 20; pp. 195-216; 1993.